Solid State Ionics 221 (2012) 1–5

Contents lists available at SciVerse ScienceDirect

Solid State Ionics

journal homepage: www.elsevier.com/locate/ssi

Mechanochemical synthesis of Li-argyrodite Li_6PS_5X (X = Cl, Br, I) as sulfur-based solid electrolytes for all solid state batteries application

Sylvain Boulineau, Matthieu Courty, Jean-Marie Tarascon, Virginie Viallet *

LRCS, CNRS-UMR7314 Université de Picardie Jules Verne, 33 Rue Saint Leu 80039, Amiens, France

ARTICLE INFO

Article history:
Received 9 February 2012
Received in revised form 5 June 2012
Accepted 5 June 2012
Available online 23 June 2012

Keywords:
All solid state batteries
Lithium battery
Solid electrolytes
Mechanical milling
Argyrodite
Ionic conductivity

ABSTRACT

Highly ion-conductive Li_6PS_5X (X = Cl, Br, I) Li-argyrodites were prepared through a high-energy ball milling. Electrical and electrochemical properties were investigated. Ball-milled compounds exhibit a high conductivity between 2 and 7×10^{-4} S/cm with an activation energy of 0.3–0.4 eV for conduction. These attractive properties were attributed to the spontaneous formation of crystallized Li-argyrodite during ball-milling. An optimization of milling time led to a conductivity of 1.33×10^{-3} S/cm for the Li_6PS_5Cl phase with an electrochemical stability up to 7 V vs. lithium. An all solid state $LiCoO_2$/Elec./In lithium ion battery using ball-milled Li_6PS_5Cl as electrolyte was successfully assembled, and its room temperature performance is reported.

1. Introduction

For the past two decades, intensive research on lithium ion battery technology attempted to optimize safety and durability issues linked with the use of liquid electrolytes that may induce sizeable risks of fire and explosion in these high energy density electrochemical systems. In this respect, the so-called "all solid state" batteries, built around non-flammable solid electrolytes, are recognized as good alternatives. Therefore, their development requires the use of an electrolyte showing high lithium ionic conductivity at ambient temperature with high electrochemical stability. A few of them, based on sulfides glasses (Li_2S–P_2S_5 systems), were reported by Hayashi to possess a good electrochemical stability (up to 10 V) and were used to fabricate batteries with reasonably high energy densities [1]. Recently, Kanno et al. reported on a new germanium-based ThioLiSICon solid electrolyte ($Li_{10}GeP_2S_{12}$) presenting a very high conductivity of 12 mS/cm at 298 K, which is comparable to or higher than standard organic liquid electrolytes [2].

Argyrodites, a class of compounds derived from the mineral Ag_8GeS_6 [3], may possess high Ag^+ or Cu^+ ion conductivities, as reported for γ-Ag_9AlSe_6 [4] or Cu_6PS_5Cl [5]. From preliminary impedance measurements, Deiseroth et al. [6] reported in 2008 on cubic Li-containing Argyrodites of general formula $Li_{7-x}PS_{6-x}X_x$ ($0\le x\le1$; X = Cl, Br, I) and with promising high values for Li^+ ion conductivities; they ranged from 10^{-2} to 10^{-3} S/cm, i.e., close to the conductivity of standard liquid electrolytes. In 2010, Pecher et al. reported values close to 4×10^{-7} S/cm for Li_6PS_5I [7]. Very recently and during the course of our study, Rao et al. independently confirmed a high ionic conductivity of 3×10^{-3} S/cm and 7×10^{-3} S/cm at 298 K for Li_6PS_5Cl and Li_6PS_5Br, respectively; both were prepared through mechanical milling and then heated for 5 h at 550 °C [8].

Besides ionic conductivity, the electrochemical stability "window" of the foreseen solid electrolyte is one of the most important criteria for battery applications. For instance, crystalline materials such as $Li_{0.29}La_{0.57}TiO_3$ [9] and $LiAl_{0.5}Ge_{1.5}(PO_4)_3$ [10] can be used as solid electrolytes, only in a specific potential window, above 1.7 V and 1.8 V vs. Li, respectively. Aware of this, Stadler et al. recently reported on the use of Br-containing Li-argyrodites compositions (samples provided by Deiseroth; 1.0×10^{-4} S/cm at 298 K, electrochemically stable from 1 to 5 V vs. Li/Li^+) in all solid state batteries using carbon coated $Li_4Ti_5O_{12}$ (c-LTO) and Li–Al alloy as active positive and negative electrode materials, respectively [11]. Such a battery using a positive electrode composite made of 70% c-LTO–30% Li_6PS_5Br poorly cycled (40% loss of initial capacity after 30 cycles) at 70 °C at a rate of C/10. This loss was ascribed to the deterioration of an interface due to the repeated volume expansion/contraction of the Li–Al alloy during lithium insertion/deintercalation.

In this study, we revisit the synthesis of Li_6PS_5X (X = Cl, Br, I) Li-argyrodites electrolytes and show, by using an arsenal of characterization techniques, how the injection of a mechanical milling step during their elaboration can positively affect their electrochemical/transport properties.

* Corresponding author. Tel.: +33 322827814; fax: +33 322827590.
E-mail address: virginie.viallet@u-picardie.fr (V. Viallet).

0167-2738/$ – see front matter © 2012 Elsevier B.V. All rights reserved.
doi:10.1016/j.ssi.2012.06.008

2. Experimental

Reagent-grade Li_2S (Sigma Aldrich 99%), P_2S_5 (Sigma Aldrich 99%) and Li*X* (Acros Organic 99%) crystalline powders were used as starting materials and mixed in stoichiometric proportions to yield global compositions of Li_6PS_5X (X = Cl, Br, I). The mechanical milling treatment was carried out for 1 g overall mass of mixed powders with 15 zirconia balls (ϕ10 mm, overall mass = 29.8 g) in a zirconia jar (45 ml). A high-energy ball milling apparatus (Pulverisette 7) was used with a rotation speed fixed at 600 rpm during 20 h via a continuous step. Indeed, previous experiences showed that intermittent millings (e.g., 2 h followed by 18 h with an intermediate grinding) lead to less conducting samples.

Samples were then annealed in an autoclave placed in a tubular furnace during 5 h at 550 °C. All processes were conducted under argon atmosphere.

For phase purity, the samples were analyzed by laboratory powder X-ray diffraction (XRD), using a Bruker D8 diffractometer with Co Kα radiation (λ_1 = 1.7892 Å, λ_2 = 1.7932 Å) equipped with a Super Speed linear detector. The profiles matching refinements of the XRD powder patterns were performed using the WinPlotr program from the FullProf suite [12].

Ionic conductivities were measured on pelletized samples obtained by cold pressing (3400 kg/cm²) on C/Li_6PS_5X/C cell. The diameter and the thickness of the pellets were 10 mm and ~1.5 mm, respectively (compactness ~80%). Impedance spectroscopy was carried out under Ar atmosphere, using a Multichannel Potentiostat (VMP 2, Biologic, France) in the frequency ranging from 200 kHz to 10 mHz.

The samples were tested for their electronic conductivity by the Hebb–Wagner polarization method [13]. Constant voltages from 2 to 5 V were applied stepwise by a potentiostat (VMP Biologic), in a stainless steel/BM sample/Li cell, which allowed measuring the current response.

Differential scanning calorimetry (DSC) experiments were carried out on a Netzsch DSC 204 F1 heat flux differential calorimeter at a heating rate of 10 K/min under a constant argon flow of 200 ml/min. The aluminum crucibles were filled with 4–5 mg of sample powder and introduced in the glove box; once in the glove box they are covered with a lid and pierced just prior to being measured.

The electrochemical properties of the Li-argyrodites were evaluated by cyclic voltammetry techniques. For such measurements, the electrolyte was sandwiched between a stainless steel disk working electrode and a lithium foil counter electrode. The potential sweeps were performed using a VMP device with a scanning rate of 1 mV/s from −0.5 V to +7 V (one sweep in 20 h).

All solid state half-cells were assembled by a cold press method (ϕ10 mm, ~0.80 mm thickness, 200 bars) with a mixture of $LiCoO_2$, argyrodite phase and VGCF (vapor growth carbon fiber) (36/54/10 ratio) as composite positive electrode and In foil (100 μm) as counter electrode. The cycling processes were performed using a VMP device with a current density of 64 μA/cm² (55.265 μA in this configuration) between 3.3 and 4.3 V (vs. Li^+/Li^0).

3. Results and discussion

3.1. Characterization of ball-milled phases

The XRD patterns of ball-milled samples shown in Fig. 1 present very broad peaks characteristic of the Li_6PS_5Cl, Li_6PS_5Br and Li_6PS_5I phases. This surprising finding simply indicates that crystallized argyrodites Li_6PS_5X phases spontaneously form, through ball-milling and without post-annealing, whatever the nature of the halogenide considered. Transmission electronic microscopy reveals the presence, besides the crystallized grains, of a Li_2S–P_2S_5–Li*X* (X = Cl, Br or I) amorphous matrix with, overall, an important instability of these materials under the electron beam.

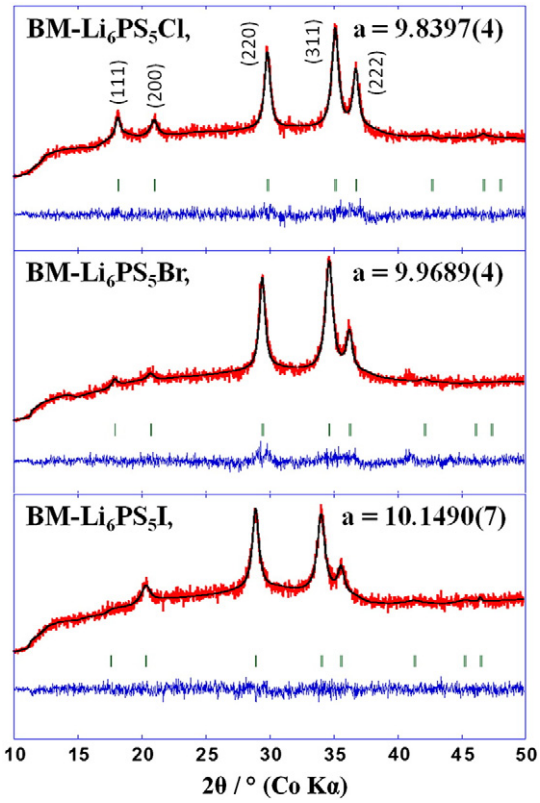

Fig. 1. Le Bail fit of BM-Li_6PS_5X (X = Cl, Br, I) XRD data.

Here, we should recall that Rao's samples obtained by mechanical milling [8] only presented diffraction peaks belonging to the Li_2S, P_2S_5 and Li*X* (X = Cl, Br or I) precursor phases. Such a difference is most likely rooted in the energetic of the ball-milling process. Rao's ball-milling had been performed in an agate jar containing 15 agate balls of ϕ10 mm corresponding to an overall mass of 13.9 g. We used zirconia jar and balls; 15 balls of ϕ10 mm correspond to an overall mass of 29.8 g. Bearing in mind that heavier balls result in more energetic impacts during milling at equal diameters [14,15], we can deduce that our ball-milling process due to the use of zirconia balls (ρ = 5.7 g/cm³) instead of agate balls (ρ = 2.65 g/cm³) was more energetic. We believe this is the reason why we could directly prepare highly crystallized Li-argyrodite phases through a simple ball-milling procedure.

The XRD powder patterns were successfully refined in a cubic cell (SGF-43m) with lattice parameters of 9.8397(4), 9.9689(4) and 10.1490(7) Å for chloride, bromide and iodide, respectively. They are in good agreement with those given in ICSD files (Li_6PS_5Br: 418488, Li_6PS_5I: 418489, Li_6PS_5Cl: 418490). The unit cell volumes were shown, as expected, to increase – $V(Li_6PS_5Cl) < V(Li_6PS_5Br) < V(Li_6PS_5I)$ – with increasing the ionic radii of the halogenide ($R_{Cl^-} < R_{Br^-} < R_{I^-}$). The isotropic peak broadening refinements led to crystallite sizes in the range of 15 nm as deduced from the Scherrer equation implemented in the FullProf suite [12]. These argyrodite phases prepared by mechanical milling will be labelled from hereafter as "BM phases" (BM = ball-milled) as opposed to the annealed ones described in the second part of this section.

The total electronic conductivity (electron + hole) is 2.6×10^{-8} (Li_6PS_5Br), 6.4×10^{-9} (Li_6PS_5Cl) and 2.4×10^{-8} S/cm (Li_6PS_5I) using the Hebb–Wagner polarization method [13]. On the other hand, respective ionic conductivities at 298 K of 6.2×10^{-4}, 4.6×10^{-4} and 1.9×10^{-4} S/cm for bromide-, chloride- and iodide-containing phases were calculated from the impedance plots measured on C/BM–Li_6PS_5X/C cells at room temperature (Fig. 2). They were simply taken as the resistances values corresponding to the intercept of the linear fit of the

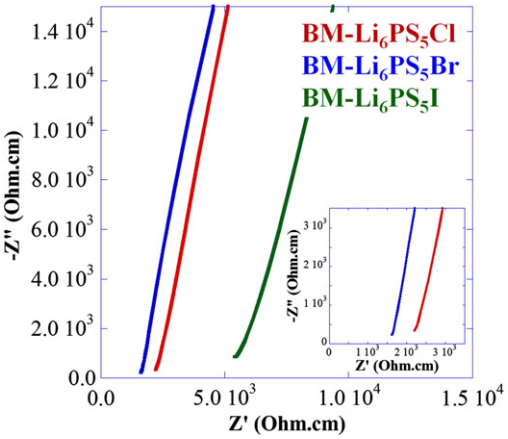

Fig. 2. Impedance spectroscopy plots, at 298 K, of C/BM-Li_6PS_5X/C cells cold pressed at 300 bar in ϕ10 mm matrix.

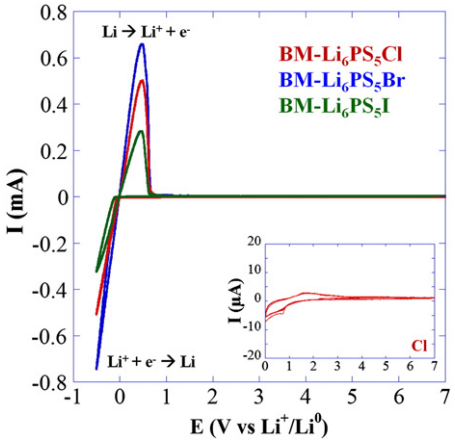

Fig. 4. Cyclic voltammetry of a stainless steel/BM-Li_6PS_5X/Li cell. Inlet: five cycles of BM- Li_6PS_5Cl sample.

Warburg curve with the *x*-axis (e.g., when the imaginary part is equal to zero). Such values are in agreement with those reported by Deiseroth et al. for the crystallized bromide and chloride phases, but differ for the crystallized iodide phase for which a value of 10^{-7} S/cm was reported as opposed to 1.9×10^{-4} S/cm for our sample.

Besides, we should note that our chloride- and bromide-containing crystallized phases present higher conductivities (~20 times higher) than the poorly crystallized ball-milled samples obtained by Rao [8], indicating that the ionic conductivity is governed by the crystalline part of the sample. In contrast, regarding the iodide-containing samples, our results are in good agreement with those of Rao et al. suggesting that in this case the ionic conductivity is governed by the amorphous part of the sample.

Temperature-dependent ionic conductivities, as determined from the analysis of each impedance spectrum, follow an Arrhenius-type law (Fig. 3) with activation energies of 0.33, 0.41 and 0.35 eV for chloride, bromide and iodide phase, respectively (calculated for temperatures ranging from 25 °C to 150 °C). These values are a little bit higher than those reported for other sulfur-based systems for solid electrolyte applications [2,16], making their room temperature use more problematic.

Besides activation energy, another figure of merit for solid electrolytes is their electrochemical stability which was evaluated from cyclic voltammograms collected on Li/BM-Li_6PS_5X/stainless steel current collector cells (Fig. 4). Cathodic and anodic currents, observed close to 0 V, correspond to the metallic lithium deposit ($Li^+ + e^- \rightarrow Li$) and stripping ($Li \rightarrow Li^+ + e^-$), respectively. Zooming in on the micro-amps scale for chloride-containing phase exhibits a total absence of any electrochemical response for at least five cycles (inlet), which is ideal for battery application.

3.2. Characterization of annealed phases

In order to increase the amounts of crystallized phase in our samples, we chose to perform heat treatments at 550 °C for 5 h under Ar, like for the original preparation of Li-argyrodite [6]. Indeed, several heat treatments at intermediate temperatures were performed and no improvement was noted until we reached temperatures of 550 °C. The samples obtained after such annealing present narrow and intense X-ray diffraction peaks of Li-argyrodites phases indicating an enhancement of their coherent scattering domain (Fig. 5).

Additional diffraction peaks witness the presence of crystallized Li*X* (*X* = Cl, Br or I) and Li_2S impurities which had been previously spotted within the BM samples through TEM observations. Two different heating rates (10 and 25 °C/min) were used, and faster heating resulted in decreasing the amount of crystallized impurities (Fig. 5). This phenomenon could be explained by the fact that during the heat treatment, P_2S_5 at the surface turns into liquid and flow-out the pellet; a high rate of temperature enables to limit this P_2S_5 departure process, hence "forcing" the P_2S_5 to react inside the pellet in order to form the argyrodite phase. From the Scherrer equation we could deduce crystallite sizes of ~90 nm for the argyrodite phase.

DSC measurements were performed on each BM-Li_6PS_5X composition. The DSC traces (Fig. 6) reveal broad exothermic peaks having

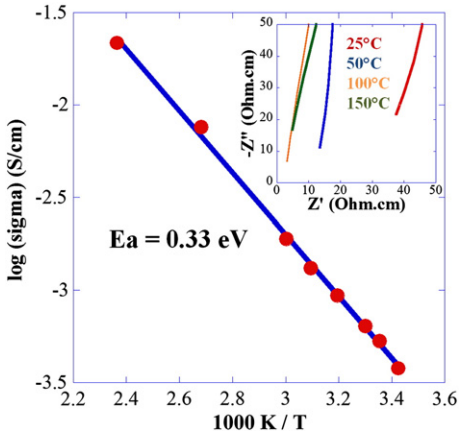

Fig. 3. Temperature dependence of the ionic conductivity for BM-Li_6PS_5Cl.

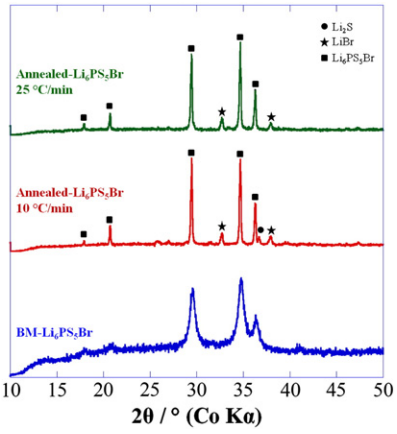

Fig. 5. Comparative XRD patterns of BM-Li_6PS_5Br before and after heat treatments. Samples were annealed at 550 °C for 5 h.

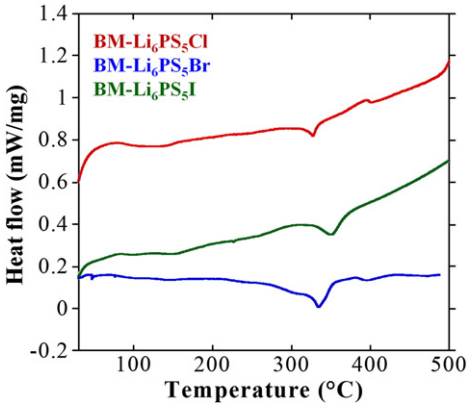

Fig. 6. DSC curves of the Li_6PS_5X (X=Cl, Br, I) samples prepared by ball-milling.

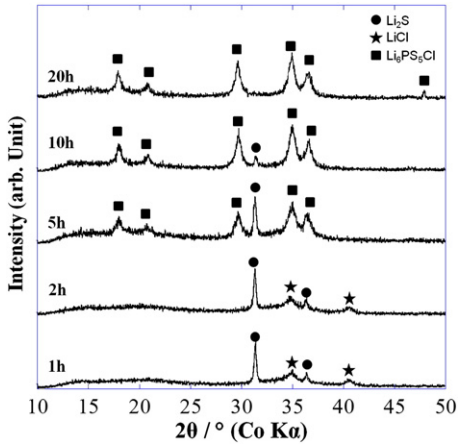

Fig. 8. XRD patterns of "Li_6PS_5Cl" samples after different times of milling.

small intensity between 100 and 400 °C together with a few barely detectable slope changes which we could not exploit reliably to deduce some basic physical characteristics, such as glass transition temperatures or other properties.

Conductivities derived from Impedance Spectroscopy performed on the annealed powders (crushed in mortar and then pressed into pellet) for the bromide and chloride phases are similar to the ones obtained for BM phases. This seems to indicate that neither the coarsening of the particles nor the increasing amount of LiX phases have an influence on the ionic conductivity. Nevertheless additional experiments, namely NMR and RAMAN spectroscopy, are in progress to grasp further insight into the understanding of the minority phase role.

In contrast, annealing the iodide-containing sample induces a huge decrease in conductivity from 2×10^{-4} to 10^{-7} S/cm (Fig. 7), this latter value being consistent with that reported by Deiseroth for his crystallized sample.

3.3. Optimization of chloride-containing phase synthesis

As the chloride-containing phase Li_6PS_5Cl shows no oxidation/reduction vs. Li in a wide voltage range, we decided to focus our study on this composition for further improvements of the synthesis procedure and electrochemical properties. We performed several ball-milling sequences of different durations (1, 2, 5, 7.5, 10, 15 and 20 h). XRD patterns were recorded after each experiment (Fig. 8).

Only broad peaks assigned to Li_2S and LiCl were observed on the XRD patterns of the samples obtained after 1 h or 2 h of ball-milling. Upon 5 h of milling, a poorly crystalline Li_6PS_5Cl phase is observed with the remaining Li_2S. After 10–20 h of milling, the crystallized Li_2S phase has almost disappeared, and after 20 h, pure Li_6PS_5Cl is mostly obtained.

Conductivities at 298 K derived from impedance spectroscopy performed after each milling present an enhancement of the conductivity from 2×10^{-4} S/cm for 1 h to 1.33×10^{-3} S/cm for 10 h of milling. For longer durations, the conductivity then decreases (Fig. 9). We have no explanation yet to account for such an observed minimum in the ionic conductivity as the function of the milling time. Therefore, we should recall that the ball-milling time dependence of the BET surface area for ball milled samples shows similar curves, with the decrease at high ball-milling time being associated to a coalescence of divided particles having high surface tensions. BET measurements are being pursued to test whether such a BET–surface area–ionic conductivity relationship does exist.

We then chose to perform preliminary battery tests with the chloride-containing phase milled for 10 h because, out of the samples we prepared, it is the one with the highest conductivity. The first electrochemical cycle obtained from a $LiCoO_2$-based composite positive electrode and an Indium negative electrode at a rate of C/20, presents a charge capacity of 130 mAh/g of $LiCoO_2$ and a reversible capacity of ~100 mAh/g, (Fig. 10).

The loss of discharge capacity observed can be related to the formation of a passivation layer at the interface between $LiCoO_2$ and the electrolyte [17]. Moreover, one notes the small polarization of the cell (150 mV) at quite high rates (C/20).

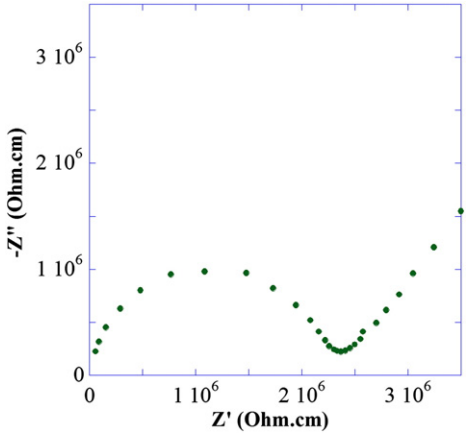

Fig. 7. Impedance spectroscopy plots, at 298 K, of annealed-Li_6PS_5I.

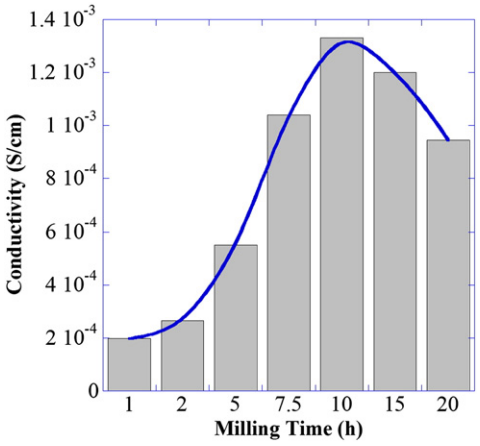

Fig. 9. Milling time dependence of ionic conductivity for Li_6PS_5Cl.

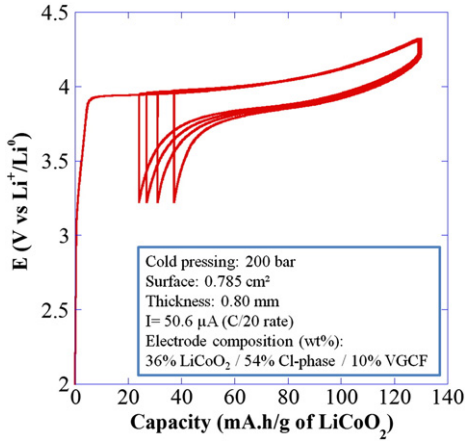

Fig. 10. Galvanostatic cycling data at 64 µA/cm² (1 Li^+ in 20 h rate) of the all-solid state half-cell $LiCoO_2$/chloride-phase/Indium ran at room temperature.

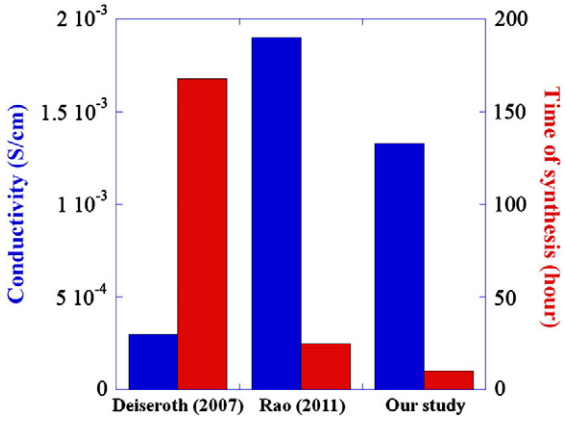

Fig. 11. Overview of data related to Li_6PS_5Cl: conductivity and synthesis time.

4. Conclusion

We have reported the elaboration, via a room temperature ball-milling process, of Li_6PS_5X (X = Cl, Br or I) argyrodites showing ionic conductivities which favorably compare to those initially reported for the same phase prepared at 550 °C by traditional ceramics syntheses [6]. The powders obtained after ball-milling present nano-sized crystallites of Li_6PS_5X in an amorphous Li_2S–P_2S_5–LiX matrix. These phases exhibit conductivities between 2 and 7×10^{-4} S/cm with an activation energy of 0.3–0.4 eV, values close to that of Thio-LISICON reported by Kanno [2]. Although annealing treatments performed on the ball-milled powders have led to an enhancement of the crystallites size of the Li_6PS_5X particles and a crystallization of LiX and Li_2S impurities, they did not result in any improvement of the overall ionic conductivity, at least for the Br- and Cl-based phases. Lastly, by tuning the ball-milling synthesis parameters we demonstrated the feasibility of obtaining, at room temperature and in a record time of 10 h (Fig. 11), a Li_6PS_5Cl phase having a conductivity of 1.33×10^{-3} S/cm at 298 K. Such a newly made solid electrolyte was implemented into an $In/Li_6PS_5Cl/LiCoO_2$ solid electrolyte battery, and the first preliminary results are encouraging for future developments.

Acknowledgements

This work was supported by the Picardy Region through the ELYSABETE project. We thank Jean-Bernard Leriche for designing the high-temperature impedance cells under controlled atmosphere, Christian MASQUELIER and Mathieu MORCRETTE for their precious advices and for proofreading this study, and Vincent SEZNEC for his fruitful help and discussion.

References

[1] A. Hayashi, K. Minami, J. Solid State Electrochem. 14 (2010) 1761–1767.
[2] N. Kamaya, et al., Nat. Mater. 10 (2011) 682–686.
[3] A. Weisbach, Neues Jahrb. Mineral. 2 (1886) 67–71.
[4] E. Gaudin, H.J. Deiseroth, T. Zaiß, Z. Kristallogr. 216 (2001) 39–44.
[5] A. Gagor, A. Pietrasko, J. Solid State Chem. 181 (2008) 777–782.
[6] H.J. Deiseroth, et al., Angew. Chem. 120 (2007) 767–770.
[7] O. Pecher, et al., Chem. Eur. J. 16 (2010) 8347–8354.
[8] R.P. Rao, S. Adams, Physica Status Solidi (a) 208 (2011) 1804–1807.
[9] P. Birke, R.A. Huggins, W. Weppner, J. Electrochem. Soc. (1997) 144–167.
[10] A. Aboulaich, et al., Adv. Energy Mater. 1 (2011) 179–183.
[11] F. Stadler, et al., ECS Trans. 25 (2010) 177–183.
[12] R. Delhez, E.J. Mittenmeijer (Eds.), WinPLOTR: a Windows tool for powder diffraction patterns analysis Materials Science Forum, Proceedings of the Seventh European Powder Diffraction Conference (EPDIC 7), 2000, pp. 118–123.
[13] B.J. Neudecker, W. Weppner, J. Electrochem. Soc. 143 (1996) 2198–2203.
[14] C. Suryanarayana, Prog. Mater. Sci. 46 (2001) 1–184.
[15] M. Abdellaoui, E. Gaffet, J. Comput. Phys. 209 (1994) 351–361.
[16] K. Minami, A. Hayashi, M. Tatsumisago, J. Ceram. Soc. Jpn. 118 (2010) 305–308.
[17] T. Minami, Solid State Ionic for Batteries, Springer-Verlag, 2005.